Complete functional rescue of the ABCA1$^{-/-}$ mouse by human BAC transgenesis

Jonathan M. Coutinho,[1,*] Roshni R. Singaraja,[1,*] Martin Kang,[*] David J. Arenillas,[*] Lisa N. Bertram,[*] Nagat Bissada,[*] Bart Staels,[†] Jean-Charles Fruchart,[†] Catherine Fievet,[†] Ann M. Joseph-George,[§] Wyeth W. Wasserman,[*] and Michael R. Hayden[2,*]

Centre for Molecular Medicine and Therapeutics,* Department of Medical Genetics, University of British Columbia, Vancouver, British Columbia V5Z 4H4, Canada; Institut Pasteur de Lille,† U545 Institut National de la Santé et de la Recherche Médicale, Lille Cedex, France; and Centre for Applied Genomics,§ The Hospital for Sick Children, Toronto, Ontario M5G 1X8, Canada

Abstract **Humanized mouse models are useful tools to explore the functional and regulatory differences between human and murine orthologous genes. We have combined a bioinformatics approach and an in vivo approach to assess the functional and regulatory differences between the human and mouse ABCA1 genes. Computational analysis identified significant differences in potential regulatory sites between the human and mouse genes. The effect of these differences was assessed in vivo, using a bacterial artificial chromosome transgenic humanized ABCA1 mouse model that expresses the human gene in the absence of mouse ABCA1. Humanized mice expressed human ABCA1 protein at levels similar to wild-type mice and fully compensated for cholesterol efflux activity and lipid levels seen in ABCA1-deficient mice. Liver X receptor agonist administration resulted in significant increases in HDL values associated with parallel increases in the hepatic ABCA1 protein and mRNA levels in the humanized ABCA1 mice, as seen in the wild-type animals. Our studies indicate that despite differences in potential regulatory regions, the human ABCA1 gene is able to functionally fully compensate for the mouse gene. Our humanized ABCA1 mice can serve as a useful model system for functional analysis of the human ABCA1 gene in vivo and can be used for the generation of potential new therapeutics that target HDL metabolism.**—Coutinho, J. M., R. R. Singaraja, M. Kang, D. J. Arenillas, L. N. Bertram, N. Bissada, B. Staels, J-C. Fruchart, C. Fievet, A. M. Joseph-George, W. W. Wasserman, and M. R. Hayden. **Complete functional rescue of the ABCA1$^{-/-}$ mouse by human BAC transgenesis.** ***J. Lipid Res.*** **2005.** 46: **1113–1123.**

Supplementary key words ATP binding cassette type A1 • humanized mouse • bacterial artificial chromosome • phylogenetic footprinting • liver X receptor • transcription factor binding site

The majority of mammalian cells are unable to metabolize cholesterol and rely on the reverse cholesterol transport (RCT) pathway to remove excess cellular cholesterol. RCT encompasses the efflux of cholesterol from the plasma membrane to HDL particles, which deliver the cholesterol to the liver, where it is secreted into the bile or used for bile acid synthesis. Alternatively, the liver can resecrete cholesterol to the body in the form of VLDL or store it for later use (1).

A significant advance in understanding HDL metabolism was achieved after the discovery that mutations in the ABCA1 gene are the cause of Tangier disease, a disorder that is characterized by a near absence of plasma high density lipoprotein cholesterol (HDL-C), the accumulation of cholesteryl esters, and an increased incidence of cardiovascular disease (2–5). ABCA1 plays an important role in the initiation of the RCT pathway by effluxing cellular cholesterol onto nascent HDL particles (6–8). In addition, ABCA1 has been implicated in several other biological processes, including apoptosis (9), inflammation (10), and the secretion of cytokines (11).

Studies in both humans and mice have shown that ABCA1 is expressed ubiquitously (12, 13). Important functional sites of expression appear to be the liver and macrophages (14). Overexpression of ABCA1 in the liver results in an increase in plasma HDL-C levels, indicating that liver ABCA1 is a significant contributor to plasma HDL-C levels (15, 16). This hypothesis was recently validated by the finding that targeted disruption of ABCA1 in the mouse liver results in a severe reduction in HDL-C lev-

Abbreviations: apoB, apolipoprotein B; BAC, bacterial artificial chromosome; CETP, cholesteryl ester transfer protein; CYP7A1, cholesterol 7α-hydroxylase; FISH, fluorescent in situ hybridization; HDL-C, high density lipoprotein cholesterol; LXR, liver X receptor; PPARα, peroxisome proliferator-activated receptor α; RCT, reverse cholesterol transport; RXR, retinoid X receptor; TFBS, transcription factor binding site.

[1] J. M. Coutinho and R. R. Singaraja contributed equally to this work.

[2] To whom correspondence should be addressed.
e-mail: mrh@cmmt.ubc.ca

Manuscript received 21 December 2004 and in revised form 15 March 2005.

Published, JLR Papers in Press, March 16, 2005.
DOI 10.1194/jlr.M400506-JLR200

els (17). In contrast, the contribution of macrophage ABCA1 to plasma HDL-C levels is low (18). Instead, ABCA1 activity in macrophages can contribute significantly to the susceptibility to atherosclerosis (10, 19).

Important insights into the function of ABCA1 in HDL metabolism have been derived from mouse studies (15, 16, 19–26). However, it is uncertain whether results obtained in mice can be translated directly to humans. Humans and mice differ considerably in many aspects of lipoprotein metabolism. Mice rely mostly on HDL to transport cholesterol, whereas in humans this is predominantly carried out by apolipoprotein B (apoB)-containing lipoproteins. Furthermore, mice lack the cholesteryl ester transfer protein (CETP), which promotes the exchange of cholesterol and triglycerides between lipoprotein classes and is an important enzyme in human HDL metabolism (27). Finally, even though there is a high level of sequence conservation between the human and mouse ABCA1 proteins (~90%), this does not exclude the possibility that there are important regulatory differences between these genes (28, 29).

Humanized mouse models are a useful tool to explore the functional and regulatory differences between human and mouse orthologous genes. The value of these models, in which the mouse gene is replaced by the human gene, lies predominantly in the possibility of expressing the human gene of interest under the control of its endogenous promoter. Studies using this technique have revealed important differences between human-mouse orthologous gene pairs. One study found that mice humanized for peroxisome proliferator-activated receptor α (PPARα), unlike wild-type mice, are resistant to the development of PPARα agonist-induced liver cancer (30). This was attributable to the fact that, in contrast to mice, human PPARα does not activate genes involved in hepatocellular proliferation, which is surprising considering the high level of sequence conservation between the human and mouse PPARα proteins (92%). Similarly, mice that are humanized for the Friedreich ataxia gene have a considerably different expression pattern than mice carrying the wild-type gene, with the human gene being expressed at much higher levels in the brain, liver, and skeletal muscle, indicating a regulatory variation between the human and mouse genes (31). A study comparing expression profiles of a large number of orthologous gene pairs recently confirmed that differences in gene expression are abundant between human and mouse (28). Finally, by using a humanized mouse model, Chen et al. (32) showed that the human cholesterol 7α-hydroxylase (CYP7A1) gene is unresponsive to liver X receptor (LXR) regulation. This was attributable to a missing LXR/retinoid X receptor (RXR) binding site in the promoter of the human CYP7A1 gene, which is present in the mouse gene.

In the present study, we have used a combined bioinformatics and in vivo approach to explore the regulatory and functional differences between the human and mouse ABCA1 genes. First, we performed a computational analysis of the regulatory regions of the human and mouse genes to search for potential differences in transcription factor binding sites (TFBSs). Next, we generated a humanized ABCA1 mouse model that expresses endogenously regulated human ABCA1 on a mouse ABCA1-deficient ($ABCA1^{-/-}$) background. We determined whether the human gene was able to rescue the phenotype of the $ABCA1^{-/-}$ mice and elucidated any differences in the level of expression, function, or regulation of ABCA1 between the humanized and wild-type control mice.

METHODS

Phylogenetic footprinting

The ABCA1 gene was analyzed to delineate segments of potential regulatory importance within or adjacent to the gene. The genomic sequences for both the human and mouse genes were obtained from the University of California Santa Cruz (UCSC) Genome Browser (33) (http://www.genome.ucsc.edu/), using human assembly 34 (July 2003) and mouse assembly 32 (October 2003). Sequences corresponding to 25,123 bp upstream of the annotated first exon were retrieved, corresponding to human chromosome 9 positions 103,030,000 to 103,095,397 and mouse chromosome 4 positions 52,812,000 to 52,861,230. The sequences were aligned using the ORCA progressive global sequence alignment program (34). Phylogenetic footprint plots were generated corresponding to 100 bp windows of the human sequence. Each window displays the percentage of human nucleotides aligned to identical nucleotides in the mouse sequence.

Regulatory potential scores

Regulatory potential scores (35) were obtained from the UCSC Genome Browser. These scores reflect the likelihood that a conserved segment contributes to the regulation of gene transcription. In short, it identifies blocks of identical nucleotides separated by blocks of variant nucleotides within an alignment under the expectation that regions containing TFBSs will exhibit such a punctate pattern of nucleotide identity.

TFBS prediction

TFBSs were predicted using the JASPAR database (www.cisreg.ca) of transcription factor binding profiles according to the protocols described by Lenhard et al. (36). Weight matrix thresholds of 80% were applied to the predictions. Conservation filtering restrained predictions to regions of 75% nucleotide identity between human and mouse.

LXR binding site prediction

The nuclear receptor LXR has been documented to bind preferentially to direct repeats of nuclear receptor half-sites separated by four nucleotides, termed DR4 elements (37). Candidate DR4 sites were predicted using the NHRscan web service (38) (www.cisreg.ca).

Generation of humanized ABCA1 mice

Bacterial artificial chromosomes (BACs) containing the ABCA1 gene were identified by screening high-density BAC grid filters from a human BAC library (RPC-11). BAC RP11-32H03 was selected, and BAC transgenic mice were generated on a C57BL/6xCBA background as described previously (20). The 5′ end of BAC 32H03 is at position −25,122 from the start of exon 1, and the 3′ end is at position +4,132 from the end of exon 50 (**Fig. 1**). Transgenic mice heterozygous for the human ABCA1 gene and backcrossed to C57BL/6J(N5) were crossed to $ABCA1^{-/-}$ mice on a pure DBA background. The resulting BAC^{+} $ABCA1^{+/-}$ mice were backcrossed to create BAC^{+} $ABCA1^{-/-}$ mice, thus gen-

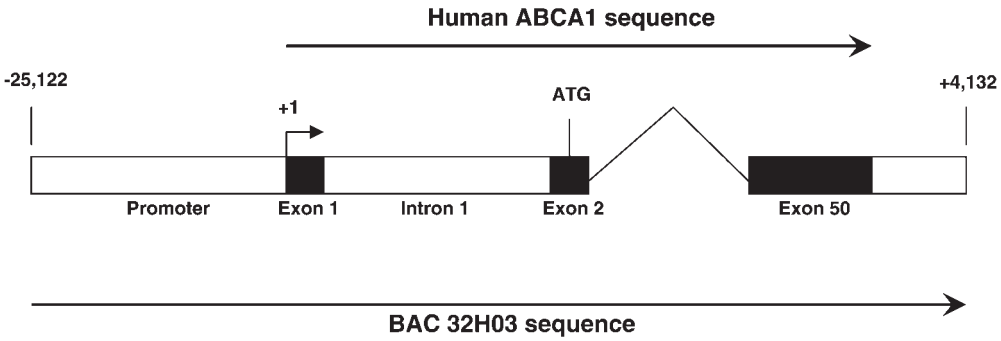

Fig. 1. Scheme of bacterial artificial chromosome (BAC) 32H03. BAC 32H03 was used to generate the humanized ABCA1 mice. The BAC starts 25,122 bp upstream of exon 1 and ends 4,132 bp downstream of exon 50, thus containing the complete genomic sequence of the human ABCA1 gene, including the promoter and the 3′ untranslated region.

erating humanized ABCA1 mice on a mouse ABCA1$^{-/-}$ background.

Southern blotting

DNA from transgenic mice and human control DNA were isolated using Qiagen DNeasy spin columns and digested with *Eco*RI (New England Biolabs). Quantities of 2.5, 5.0, 7.5, and 10.0 μg of DNA were digested and separated on a 0.8% agarose gel. The gel was transferred to a Hybond N+ membrane (Amersham), and the blots were prehybridized at 42°C for 4.5 h in 1% BSA, 1% Ficoll, 250 mM Tris-HCl (pH 7.5), 0.5% sodium pyrophosphate, 5% SDS, 1% polyvinylpyrrolidone, 50% formamide, and 10% dextran sulfate. An ~4 kb Kpn fragment of a cDNA construct of ABCA1 was used as a probe for the Southern blot. The probe was labeled with [^{32}P]dCTP using the Rediprime II DNA labeling kit (Amersham) and subsequently purified using NICK columns (Amersham). The purified probe was boiled and added to blots to hybridize overnight at 42°C. Blots were then washed twice in 2× SSC/0.1% SDS for 30 min at room temperature followed by four 30 min washes in 0.1× SSC/0.1% SDS. The blot was exposed to film at −70°C overnight.

Fluorescent in situ hybridization

Splenocytes were extracted from spleens of humanized and wild-type mice. Cells were cultured for 72 h at 37°C in RPMI 1640 medium supplemented with 10% fetal bovine serum and mitogenic lipopolysaccharide (final concentration, 20 μg/ml). Cultures were exposed for 15 min to Colcemid (final concentration, 0.05 μg/ml) and harvested according to standard cytogenetic protocol, using hypotonic 0.075 M KCl and Carnoy's fixative. Metaphase preparations were made by dropping the fixed cell suspension onto precleaned slides in a Thermotron, and these were aged overnight at 55°C before G-banding using 2% trypsin followed by staining with Leishmann/Giemsa stain. At least 10 metaphase spreads for each sample were imaged using bright-field microscopy, and the coordinates of these were recorded for metaphase relocation after fluorescent in situ hybridization (FISH). Before FISH was performed, slides were destained with Carnoy's fixative, rehydrated with an ethanol series, pretreated with 2× SSC at 37°C, then postfixed with 1% formaldehyde/PBS/$MgCl_2$ and washed in PBS. Metaphases were denatured for ~30 s in 70% formamide/SSC at 70°C and dehydrated with ethanol. Genomic DNA was isolated from BAC clones and labeled with Spectrum green (green; RP23-161K8, AC111090; mouse chromosome 5 control probe) and digoxigenin (red; RP11-32H03; transgene). Probes were denatured for 5 min at 75°C and hybridized to slides overnight at 37°C. After hybridization, slides were washed and incubated with detection solution for 30 min at 37°C, rinsed, and stained with 4′,6-diamino-phenylindole. Previously imaged G-banded metaphases were relocated, examined using fluorescence microscopy, and reimaged.

Lipid and HDL subparticle analysis

Plasma and lipoprotein lipid concentrations were determined as described previously (21). Apolipoprotein levels were measured by immunonephelometry using mouse polyclonal antibodies. Preβ- and α-HDL were separated by a double immunoelectrophoresis technique according to their mobility. The first separation was achieved by running 4 μl of each plasma sample on an agarose gel (1%, w/v) for 2 h at 500 V. The second one was obtained by migration of each lane including the separated proteins on a 1% (w/v) agarose gel containing mouse anti-apoA-I immunoserum for 3 h at 50 V. Finally, the gel was washed, dried, and stained with Coomassie blue R250 (0.5%, w/v). The peaks corresponding to the HDL fractions were quantified by scanning (Scan Wise 1.2). The results are expressed in percentage of apoA-I contained in each HDL subfraction.

Protein analysis

Protein levels were determined by Western blotting. Tissue lysates were prepared as described previously (20). Thioglycollate-elicited peritoneal macrophages were incubated overnight in DMEM containing 10% FBS and L-glutamine and harvested the next day for Western immunoblotting, as described previously (20). Forty to 80 μg of protein, as determined by Lowry assay (39), was separated on a 7.5% polyacrylamide gel and transferred overnight to a polyvinylidene difluoride membrane (Millipore). Membranes were probed with the PEP4 polyclonal rabbit antibody for detection of ABCA1 and anti-glyceraldehyde phosphate dehydrogenase (Chemicon) as a loading control.

Cholesterol efflux assay

Mouse peritoneal macrophages were isolated 3 days after injection with 3% thioglycollate as described previously (20). Cells were loaded for 24 h with 1 μCi/ml [^{3}H]cholesterol (Perkin-Elmer) and subsequently allowed to efflux for 24 h in DMEM containing 0.2% defatted BSA (Sigma) in the presence or absence of 10 μg/ml apoA-I (Calbiochem). Cholesterol efflux was calculated as the total counts in the media divided by the sum of the counts in the media and cells.

LXR agonist feeding experiment

Mice were orally fed a LXR agonist (T-0901317; Sigma) for 5 days at a dose of 10 mg/kg/day. The LXR agonist was dissolved

in DMSO at a concentration of 50 mg/ml. Before use, the LXR agonist was diluted 1:1 in Chremophor (Sigma) and then 1:10 in 5% mannitol-water. On the morning of the 6th day, blood was collected by saphenous vein bleed. Plasma lipids were analyzed using commercial kits (Sigma). Primary hepatocytes were isolated as described previously (40). Cells were seeded at a density of 500,000 cells/well on a six-well plate. The next day, cells were treated for 24 h with T-0901317. Cell lysates were prepared and Western blotting was performed as described above.

Gene expression analysis of human ABCA1

Total murine RNA from liver was extracted using the RNeasy Mini Kit (Qiagen, Mississauga, Ontario, Canada) according to the manufacturer's instructions. Reverse transcription on 5 μg of the isolated RNA was carried out using the SuperScript First-Strand Synthesis System for RT-PCR (Invitrogen Life Technologies, Carlsbad, CA) according to the manufacturer's instructions. A multiplex PCR of 18S and human ABCA1 cDNA was carried out using the following primers: Ex3F (hABCA1), CAAACATGT-CAGCTGTTACTGGAAG; and Ex4R (hABCA1), GAGCCTCCC-CAGGAGTCG. 18S primers were purchased commercially (Ambion, Inc., Austin, TX). A cycling condition of 94°C for 30 s, 60°C for 45 s, and 72°C for 1 min was used. A total of 30 PCR cycles were carried out. Images were captured on a Gel Doc 1000 system (Bio-Rad, Hercules, CA) and analyzed using quantitation software (Bio-Rad Quantity One). Values of human ABCA1 are ratios with the corresponding 18S bands.

Statistical analysis

All statistical analyses were performed using the unpaired two-tailed Student's *t*-test.

RESULTS

Computational analysis of the human and mouse ABCA1 genes

In an effort to delineate potential *cis*-regulatory segments in the ABCA1 gene, a comprehensive bioinformatics analysis was performed. Using methods aimed to improve the specificity of predictions (41), the analysis coupled phylogenetic footprinting with profile-based searches for TFBS. Preliminary analyses, in which the entire gene including 50 kb upstream of exon 1 was screened, indicated

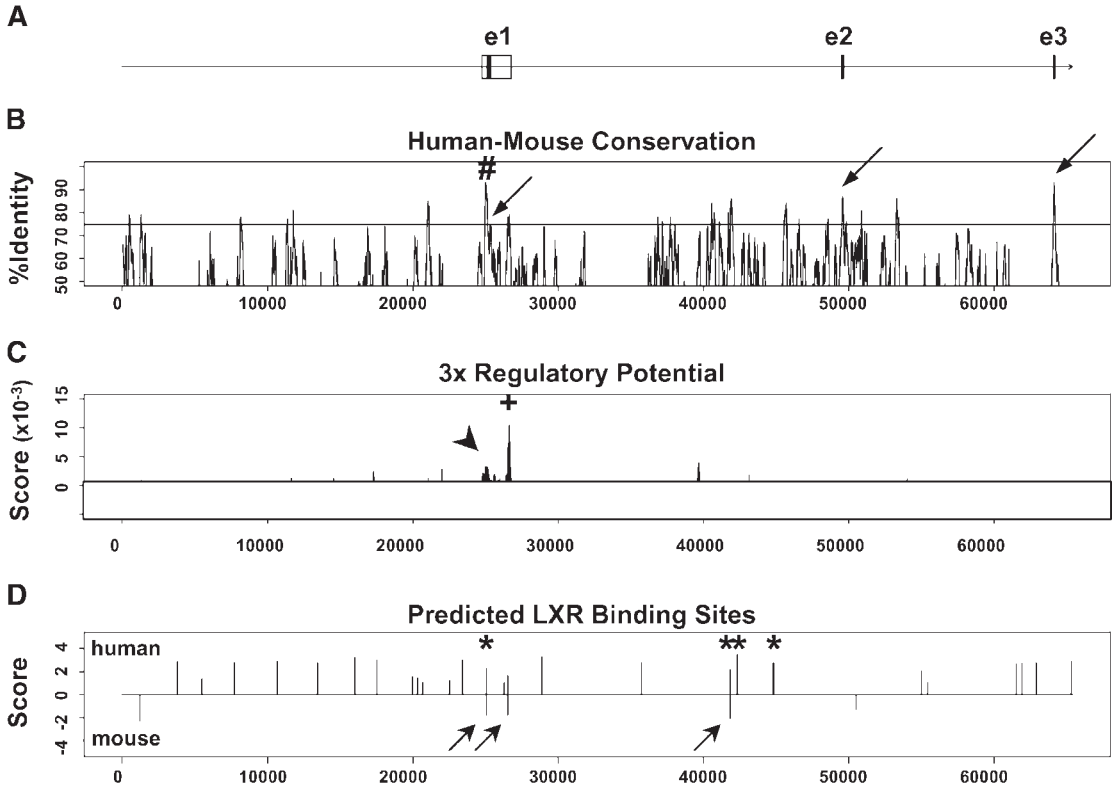

Fig. 2. Gene regulation bioinformatics analysis. The human and mouse ABCA1 gene sequences were analyzed to define candidate regulatory regions. The displayed segment of the ABCA1 gene corresponds to human chromosome 9 positions 103,030,000 to 103,095,397 (assembly version 34, July 2003), which starts 25 kb upstream of the first exon and ends 12 kb downstream of exon 3. A: Graphic display of exon positions (black boxes) and a CpG island surrounding exon 1 (white box). B: Phylogenetic footprint depicts the percentage of human nucleotides identical to mouse nucleotides in a sliding 100 bp window drawn across a global sequence alignment. A threshold line is displayed at 75% identical nucleotides. Arrows indicate the conservation peaks of the exons, and the conservation peak of the known ABCA1 promoter is indicated by a number sign. C: Three-way regulatory potential scores suggesting the presence of clusters of transcription factor binding sites conserved between human, mouse, and rat ABCA1 sequences. The arrowhead indicates the regulatory potential peak of the known ABCA1 promoter, and the plus sign marks the position of a regulatory potential peak in intron 1 with no known regulatory function. D: Candidate liver X receptor (LXR) binding sites present in the human (top) and mouse (bottom) sequences. Each vertical line marks one LXR site. The magnitude of the lines indicates the log of the posterior probability of nuclear receptor binding reported by the NHRscan software. The arrows denote putative binding sites conserved between the human and mouse sequences, and the asterisks mark the LXR binding sites reported previously (19, 43).

that the most interesting features were restricted to the upstream region and the first and second introns (data not shown). Therefore, in subsequent analyses, only these regions were examined (**Fig. 2A**). Substantial segments of similarity were observed between the human and mouse sequences, with the greatest identity observed in the 3′ half of the first intron and the regions immediately adjacent to the first exon (Fig. 2B). These patterns suggest that ABCA1 transcriptional regulation is significantly influenced by these segments, a prediction that is supported by in vitro findings and in transgenic mice (20, 42). Santamarina-Fojo et al. (42) found that the region immediately upstream of exon 1 regulates ABCA1 expression in a cAMP- and cholesterol-dependent manner. Furthermore, Singaraja et al. (20) showed that intron 1 of the human ABCA1 gene contains a functional promoter that regulates the expression of three alternative ABCA1 transcripts.

Correspondingly, a bioinformatics technique based on the analysis of patterns of nucleotide identity between orthologous sequences delineates two potential *cis*-regulatory modules flanking the first exon (Fig. 2C). The first, situated directly upstream of exon 1, localizes to a region that has previously been identified as the ABCA1 promoter (42). The second module, the highest scoring in the ABCA1 gene, is located at the beginning of intron 1. No regulatory function has been reported in this region of intron 1. However, previous studies have identified an alternative promoter in intron 1, located closer to exon 2 (20, 26).

Phylogenetic footprinting, in combination with profiles for the prediction of TFBSs, has proven to be an effective method to delineate functional binding sites (43). Predicted TFBSs in conserved regions were abundant, but only ~20% of the candidate TFBSs within these regions were conserved between human and mouse (**Table 1**). The substantial number of species-specific TFBSs in conserved regions may be indicative of differences in the regulation of the human and mouse genes (43).

Based on the divergent composition of TFBSs in human and mouse, we analyzed the distribution of binding sites for LXR, a nuclear receptor previously demonstrated to regulate ABCA1 (44) (Fig. 2D). Of the predicted LXR binding sites, only three were conserved between human and mouse (marked by arrows). Two of these sites (marked by asterisks) have been described previously, and both were shown to have functional activity (20, 44). The third site, however, has not been described. Strikingly, the human gene sequence contained an additional 23 putative LXR binding sites, whereas the mouse sequence contained only 3 additional sites. Given the important role of LXR in regulating the expression of the ABCA1 gene, this difference in LXR binding sites could indicate significantly different regulation of the human and mouse genes. The genomic coordinates of all LXR sites are available at http://www.cisreg.ca/genes/ABCA1.

TABLE 1. Candidate TFBSs in human and mouse ABCA1 genes

Species	Total TFBSs	TFBSs in Conserved Regions	TFBSs in Conserved Regions Present in Human and Mouse	Species-Specific TFBSs in Conserved Regions
Human	17,820	931	178	753
Mouse	11,264	832	178	654

Transcription factor binding sites (TFBSs) were predicted (using the JASPAR database) in human and mouse ABCA1 genes. The specific TFBSs are reported on the ABCA1 regulatory analysis web page (http://www.cisreg.ca/genes/ABCA1). A total of 17,820 and 11,264 TFBSs were predicted in the human and mouse sequences, respectively. After selecting for TFBSs located in conserved regions, 931 and 832 TFBSs remained. Of these, 178 were present in both the human and mouse sequences. A total of 753 human TFBSs (~80% of sites in conserved regions) were not found in the mouse sequence.

Generation of humanized ABCA1 mice

A humanized ABCA1 mouse model was generated to assess the regulatory and functional differences between human and mouse ABCA1 in vivo. ABCA1 BAC transgenic mice were bred onto an ABCA1$^{-/-}$ background to create a fully humanized ABCA1 mouse model in which human ABCA1 is expressed under the control of its endogenous human promoter. The copy number of the human ABCA1 gene was assessed by Southern blotting. Equal concentrations of transgenic and human control DNA resulted in similar signal strength, indicating that both are likely to have the same ABCA1 gene copy number (**Fig. 3**).

To determine the exact chromosomal integration site, analysis using sequential G-banding to FISH was performed. The human ABCA1 BAC was labeled with digoxigenin (red signal), and a control probe for mouse chromosome 5 was labeled with Spectrum green (green signal). All metaphases analyzed from the humanized mice showed one chromosome 5 to have both red and green signals, whereas its homolog had only green signal (**Fig. 4A**). Comparison of the sequential G-banded and FISH images

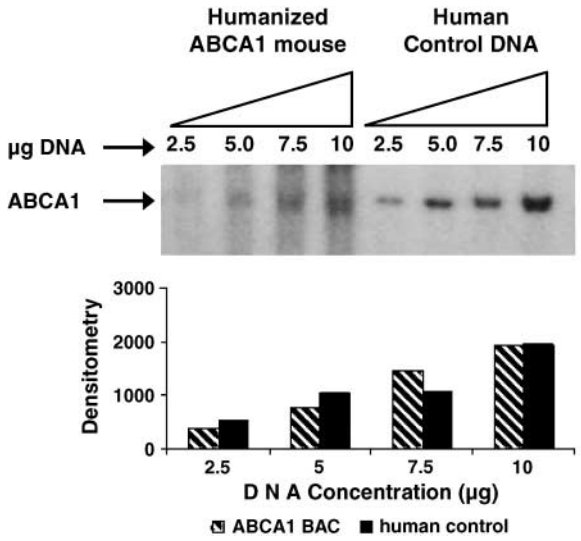

Fig. 3. Southern blotting suggests that humanized mice carry two copies of the human ABCA1 gene. Southern blotting was performed to determine the copy number of the human ABCA1 transgene. Various concentrations of DNA from the humanized ABCA1 mice and human control DNA were compared. DNA from the humanized mice and the control DNA show similar ABCA1 band intensity as determined by densitometric scanning, thus indicating that both have the same copy number.

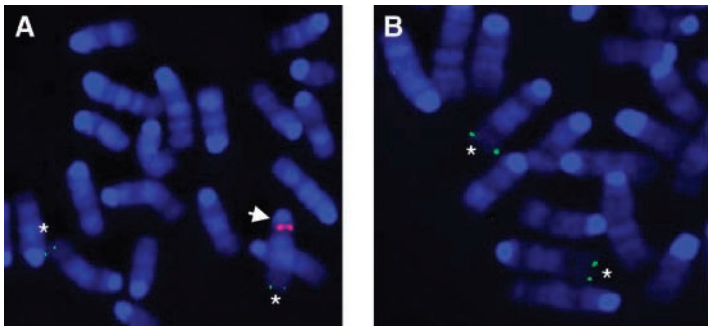

Fig. 4. Fluorescent in situ hybridization (FISH) analysis shows single-site integration of the human ABCA1 BAC at chromosome 5. Splenocytes were isolated from humanized and wild-type mice and probed for chromosome 5 (green signal) and the human ABCA1 BAC (red signal). A: Humanized mouse. The human ABCA1 BAC was detected only at one location in the humanized mice (arrow), indicating that the BAC integration had occurred at a single site. Furthermore, the BAC signal colocalizes with the green signal of the control probe for chromosome 5 (asterisks), showing that BAC has integrated into this chromosome. G-banding showed the integration site to be chromosome 5qA3/B1. B: Wild-type mouse. As a control, FISH was also performed on wild-type mice. The green signal from the chromosome 5 control probe was visualized on both homologs (asterisks), and no signal from the human ABCA1 probe was detected.

of the same metaphases enabled the location of the insertion site to be mapped to chromosome 5qA3/B1. Furthermore, the humanized mice showed only one human BAC signal, indicating that the BAC integration had occurred at a single site. Wild-type mice, used as a control, showed no human ABCA1 signal (Fig. 4B).

Humanized mice express ABCA1 protein at normal levels

ABCA1 protein levels were determined in four tissues that normally express high levels of ABCA1: liver, macrophages, spleen, and testis (12) (**Fig. 5**). No ABCA1 protein was detected in the ABCA1$^{-/-}$ mice. Slightly lower levels of ABCA1 expression were seen in humanized mice in liver, spleen, and macrophages, with slightly higher levels in testis, but these did not reach statistical significance, indicating that the expression of ABCA1 in these tissues is similar in human and mouse.

Human ABCA1 rescues functional defects of ABCA1$^{-/-}$ mice

We analyzed plasma and lipoprotein lipid phenotypes and measured cholesterol efflux in primary macrophages to determine whether the humanized mice show functional rescue of mouse ABCA1 deficiency. ABCA1$^{-/-}$ mice show a severe reduction in HDL-C and HDL-associated apolipoproteins (apoA-I, apoA-II, and apoE), whereas non-HDL-C and apoB levels are not affected (**Table 2**). In contrast, humanized mice show a complete restoration of all affected lipid values, and no difference between wild-type and humanized mice was observed. The HDL fraction was further analyzed by determining the HDL subparticle ratio (**Fig. 6**). This showed that wild-type and humanized mice have identical ratios of preβ- and α-HDL, 5% and 95%, respectively. HDL-C levels in the ABCA1$^{-/-}$ mice were too low to determine the HDL subparticle ratio. Next, cholesterol efflux was determined from primary macrophages (**Fig. 7**). No differences were observed between the efflux values of humanized and wild-type mice, whereas both had increased levels compared with ABCA1$^{-/-}$ mice ($P < 0.002$). These results indicate that human ABCA1 is functionally able to compensate for mouse ABCA1.

LXR stimulation results in a similar ABCA1 protein and HDL-C increase in humanized and wild-type mice

LXR plays a major role in the expression of the ABCA1 gene (44). Our computational analysis of the ABCA1 promoter shows that there are considerably more putative

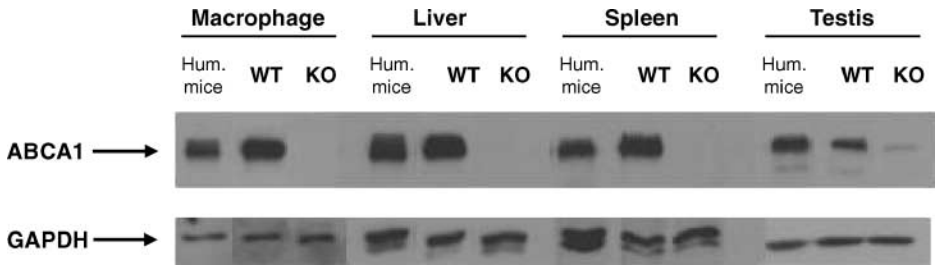

Fig. 5. Humanized mice express ABCA1 protein at normal levels. ABCA1 protein levels were determined by Western blotting in macrophage, liver, spleen, and testis (top panel). No ABCA1 protein was detected in the ABCA1$^{-/-}$ mice. Humanized ABCA1 mice show ABCA1 expression levels that are similar to wild-type levels. As a loading control, GAPDH protein levels were determined (bottom panel). Hum mouse, humanized ABCA1 mouse; KO, ABCA1$^{-/-}$ mouse; WT, wild-type mouse.

TABLE 2. Analysis of plasma lipid and apolipoprotein levels

Lipid or Apolipoprotein	ABCA1$^{-/-}$ (n = 6)	Wild Type (n = 7)	Humanized ABCA1 (n = 8)	*P* Value by Student's *t*-Test: Humanized ABCA1 vs. ABCA1$^{-/-}$	*P* Value by Student's *t*-Test: Humanized ABCA1 vs. Wild Type
Total cholesterol	52.4 (4.9)	95.7 (9.6)	97.7 (3.1)	<0.001	NS
High density lipoprotein cholesterol	5.9 (1.0)	47.9 (10.5)	48.8 (10.0)	<0.001	NS
Triglycerides	134.9 (34.6)	75.9 (16.7)	111.8 (49.3)	NS	NS
Non-high density lipoprotein cholesterol	46.4 (5.2)	47.8 (11.7)	48.9 (11.6)	NS	NS
HDL/total cholesterol ratio	0.12 (0.03)	0.50 (0.11)	0.50 (0.11)	<0.001	NS
Apolipoprotein A-I	<8%	100% (15.9)	87% (23.6)	<0.001	NS
Apolipoprotein A-II	<12%	100% (23.4)	100% (20.8)	<0.001	NS
Apolipoprotein B	115% (7.0)	100% (31.5)	107% (38.5)	NS	NS
Apolipoprotein E	40% (4.7)	100% (24.2)	101% (25.8)	<0.001	NS

Lipid values are in milligrams per deciliter. Apolipoprotein values are shown as percentages of the values of wild-type mice. Standard deviations are shown in parentheses.

LXR binding sites in the human gene than in the mouse gene, which could indicate a difference in LXR regulation. To assess this possibility in vivo, ABCA1$^{-/-}$, wild-type, and humanized mice were treated with the LXR agonist T-0901317, a known activator of ABCA1 transcription. Short-term treatment with this compound has been shown to lead to an increase in ABCA1 protein and HDL-C levels (45). As expected, ABCA1$^{-/-}$ mice showed no increase in HDL-C levels after feeding (**Fig. 8A**). Both wild-type and humanized mice, however, responded to the LXR agonist with a similar increase in HDL-C (25 and 31 mg/dl, respectively; $P < 0.001$ for ABCA1$^{-/-}$ vs. wild-type or humanized mice; $P > 0.05$ for wild-type vs. humanized mice). The effect of LXR regulation on ABCA1 protein levels was assessed by treating primary hepatocytes with the LXR agonist. Hepatocytes from both wild-type and humanized mice showed a similar increase in ABCA1 protein after LXR stimulation (Fig. 8B). It has been shown that this increase in protein levels (~2.2-fold) in wild-type mice after T-0901317 is paralleled by a significant and similar increase in ABCA1 mRNA levels (46). Similarly, the humanized mice show a 2.5-fold increase in ABCA1 mRNA levels (Fig. 8C), which is similar in magnitude to the increase in ABCA1 protein levels. Together, these data indicate that the difference in potential LXR binding elements between the human and mouse ABCA1 genes does not result in a difference in the LXR-regulated increase in ABCA1 activity.

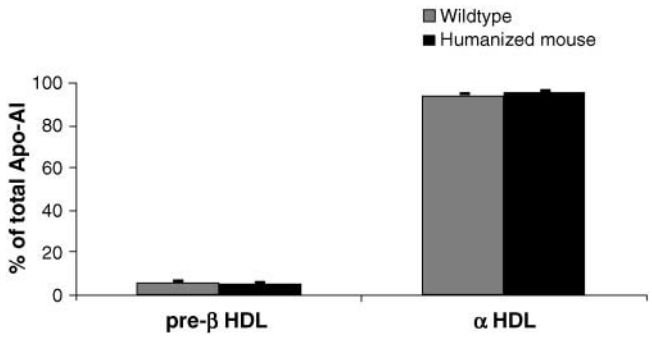

Fig. 6. HDL subparticle analysis of humanized and wild-type mice. HDL from wild-type and humanized mice was separated on an agarose gel containing anti-apolipoprotein A-I (apoA-I) immunoserum. Preβ- and α-HDL fractions were calculated by determining the percentage of apoA-I in each subfraction. The HDL levels were too low in the ABCA1$^{-/-}$ mice to determine subparticle ratios. Humanized and wild-type mice show identical ratios of preβ- and α-HDL, 5% and 95%, respectively. Error bars represent the standard deviation from the mean.

DISCUSSION

Much of our understanding of the role of ABCA1 in HDL metabolism results from studies performed in mice (15, 16, 19–26). To translate these results to humans, however, it is important to understand the level of functional and regulatory conservation between the human and mouse ABCA1 genes. Recent studies comparing other highly conserved human-mouse orthologous gene pairs have identified important differences (30–32), indicating that a high level of sequence conservation does not guarantee functional and regulatory conservation. In addition, HDL metabolism varies considerably between humans and mice, which could potentially result from or lead to differences in ABCA1 function.

To examine this, we performed a combined bioinformatics and in vivo analysis of the human and mouse ABCA1 genes. A computational analysis of the ABCA1 gene revealed several conserved putative regulatory regions, including the known ABCA1 promoter. However, we also identified extensive differences in putative TFBSs between the human and mouse genes, most notably in the number of binding sites for LXR, which could indicate a difference in gene regulation.

The findings from our computational analysis were further explored in vivo by generating a mouse model that is humanized for the ABCA1 gene. Southern blotting indicated that two copies of the human ABCA1 gene were present in the humanized mice, allowing us to directly compare our results with wild-type mice. First, we showed that humanized mice expressed ABCA1 protein at similar levels as wild-type mice. Second, introduction of the human ABCA1 gene resulted in complete functional rescue of mouse ABCA1 deficiency. Third, the LXR agonist

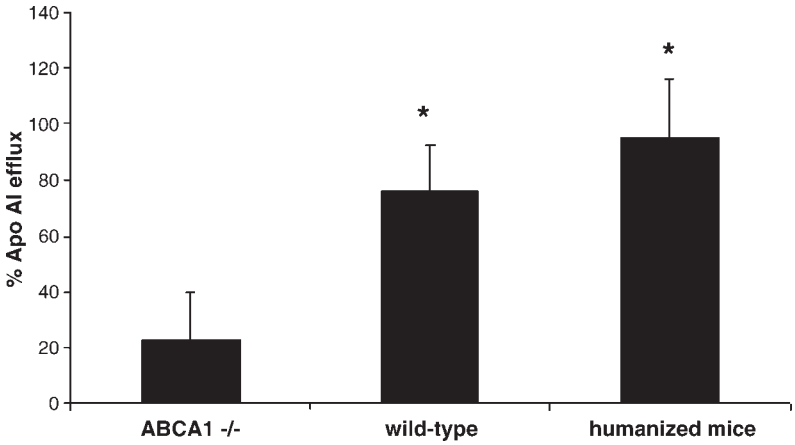

Fig. 7. Wild-type and humanized mice show increased cholesterol efflux compared with ABCA1$^{-/-}$ mice. Cholesterol efflux was performed on peritoneal macrophages from ABCA1$^{-/-}$, wild-type, and humanized mice. Efflux is significantly increased in both wild-type and humanized mice compared with ABCA1$^{-/-}$ mice ($P < 0.002$). Efflux from humanized and wild-type mice did not differ significantly from each other ($P = 0.22$). Error bars represent the standard deviation from the mean. * $P < 0.002$ compared with ABCA1$^{-/-}$.

T-0901317 resulted in significant increases in HDL values, ABCA1 protein, and ABCA1 mRNA levels in the humanized mice, similar to those seen and reported in wild-type mice (46). Thus, we observed no differences in the LXR-mediated regulation of the human and mouse genes. Therefore, the observed conservation of both the regulatory and functional characteristics of the human and mouse ABCA1 genes suggests that key regulatory and functional elements are preserved in the human and mouse sequences. It must be noted, however, that this study addressed only the tissues and conditions previously linked with important functions of ABCA1; therefore, it does not preclude differences between the regulation of the human and mouse genes in other tissues and contexts.

Qiu et al. (47) previously performed a computational analysis of the human and mouse ABCA1 genes. We, however, applied a less stringent threshold for nucleotide identity to classify segments of interest within the sequence alignment and focused on the 5′ end of the gene most likely to contain regulatory regions (48). In addition, we applied a broader set of proven bioinformatics methods, such as the analysis of regulatory potential and the promoter-wide identification of potential TFBSs in the conserved regions.

Our bioinformatics analysis shows that the human ABCA1 gene has considerably more LXR binding sites than the mouse gene. In spite of this, however, we observed a similar response to LXR stimulation in both humanized and wild-type mice, resulting in an increase in HDL levels and ABCA1 protein levels. One possible explanation for the apparent redundancy of the excess human predicted DR4 binding sites could be a limitation of the bioinformatics method. Two reports have indicated that subtle nucleotide changes adjacent to DR4 sites can have dramatic impact on the mediation of transactivation by LXR (49, 50). Still, the apparent conservation of LXR regulation indicates that the functionally important LXR binding sites are the ones that are present in both the human and mouse genes. Of the 26 LXR binding sites we identified in the human gene, only 3 are conserved in the mouse gene. Two of these sites, located in the ABCA1 promoter 5′ of exon 1 and in intron 1, have been described previously (20, 44). The third site, however, located at the 5′ end of intron 1 (1,188 bp from the end of exon 1), has not been described previously and lies in a region that has a very high regulatory potential score, suggesting functional significance.

Based on its role in the RCT pathway, increased ABCA1 activity has been shown to protect against the development of atherosclerosis. This hypothesis is supported by the finding that Tangier disease patients have an increased incidence of coronary artery disease (5). In addition, mouse studies show that specific inactivation of macrophage ABCA1 results in an increase of atherosclerosis (19), whereas overexpression of ABCA1 results in a reduction of atherosclerosis (21). Based on these findings, ABCA1 is considered to be a promising new target for the development of therapeutics (21, 51). Our humanized ABCA1 mouse model could prove to be a valuable in vivo model to test these potential therapeutic approaches. Humanized mice provide a better representation of the human physiological situation than wild-type mice, and results in these models are more likely to accurately predict whether the intervention will have the desired effect in humans (52, 53). Furthermore, the humanized ABCA1 mice can be crossed to an atherosclerosis model, such as the apoE$^{-/-}$ mouse, allowing better assessment of the effect of the drug on the development of atherosclerosis. Alternatively, the mouse model can be crossed with CETP transgenic mice, creating a model that more accurately resembles human lipoprotein metabolism (54).

Phylogenetic footprinting and regulatory sequence analysis of the ABCA1 gene indicate the presence of three major candidate regulatory regions. Two of these regions have previously been shown to play an important role in ABCA1 regulation, emphasizing the utility of this method to identify regulatory sequences. The region immediately upstream of exon 1 shows the highest level of nucleotide identity (82% across the 216 bp segment) and has previously been identified as the ABCA1 promoter (42). Several TFBSs have been mapped in this region, including a LXR/RXR binding site that has been shown to have functional activity (44). The second region with a known regulatory function is located in the 3′ half of intron 1. The regulatory activity of this region has been investigated in

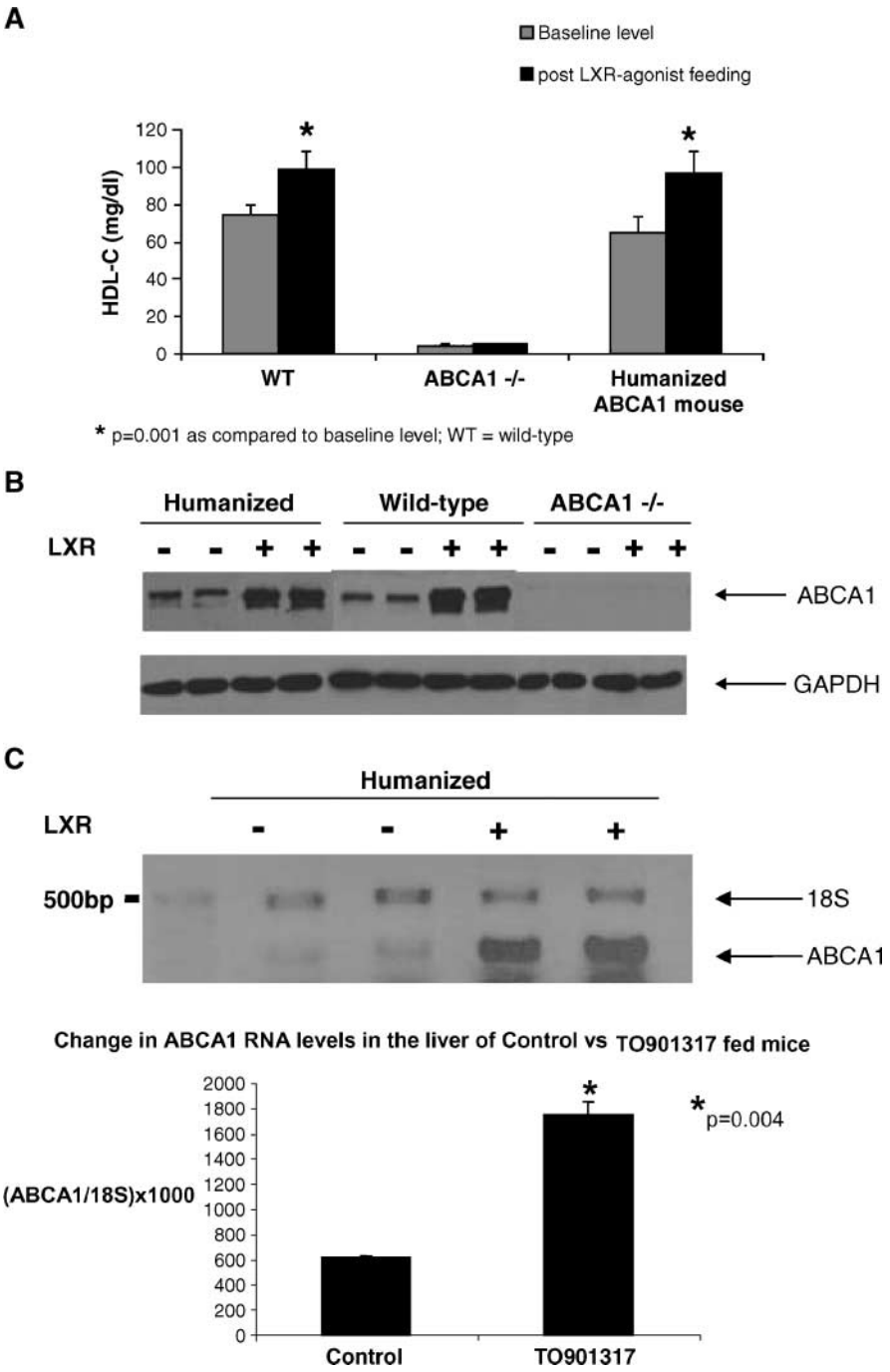

Fig. 8. Wild-type and humanized mice show a similar increase in high density lipoprotein cholesterol (HDL-C) and ABCA1 protein in response to stimulation with a LXR agonist. A: Wild-type, ABCA1$^{-/-}$, and humanized ABCA1 mice were fed an LXR agonist for 5 days (minimum of four mice per group). Blood was collected at baseline and after the feeding period, and HDL-C levels were measured. Both wild-type and humanized ABCA1 mice showed similar increases in HDL-C in response to the LXR agonist. B: Western blot of primary hepatocytes. Hepatocytes were isolated from humanized, wild-type, and ABCA1$^{-/-}$ mice and treated overnight with an LXR agonist. No ABCA1 protein was observed in ABCA1$^{-/-}$ mice. Humanized and wild-type mice show a similar increase in ABCA1 protein. The bottom panel shows the GAPDH signals used as a loading control. C: RNA levels from the livers of humanized mice treated for 5 days with an LXR agonist. Humanized mice show a significant increase in human ABCA1 mRNA levels ($P = 0.004$) when treated with the LXR agonist T-0901317. 18S mRNA signals were used as a loading control. Error bars represent the standard deviation from the mean.

two studies using BAC transgenic mice that lack the ABCA1 promoter and exon 1 (20, 26). Both studies indicate that this part of intron 1 can act as an alternative promoter and revealed several novel ABCA1 transcripts that each contained an alternative exon 1 (20). A third region of interest is located in the 5′ end of intron 1, proximal to the first exon. No regulatory function has been mapped to this region; however, several of our findings suggest a potential function for this segment. First, the sequence is highly conserved between human and mouse. Second, the location is consistent with observations that functional TFBSs tend to be located within 2000 bp of the transcription start site (48). Third, this region has the highest regulatory potential score of the ABCA1 gene. Finally, like the other two regions, this segment contains a binding site for LXR that is conserved between the human and mouse genes.

In conclusion, our humanized mouse model shows that despite a large difference in potential TFBSs in the tissues examined, human ABCA1 is able to compensate for mouse ABCA1 deficiency with regard to the levels of expression, function, and regulation. This finding underscores the level of conservation of ABCA1 between mouse and human and substantiates the use of the mouse as an experimental model to assess the function of human ABCA1 in vivo.

The authors thank Omar Francone for generously providing the ABCA1$^{-/-}$ animals used in this study. They are also very grateful to Braydon Burgess and all of the members of the animal unit for their assistance in generating and caring for the transgenic mice. The authors also thank Martin Li for performing the FISH experiments. They are especially grateful to Jaap Twisk, Liam Brunham, Marcia Macdonald, Cheryl Wellington, John Kastelein, and the members of our research groups for their intellectual input. This work was supported by the Dr. Saal van Zwanenberg Foundation (J.M.C.; Fellowship 03-019) and The Netherlands Heart Foundation (J.M.C.; Grant 2003SB106) as well as by funding from the Canadian Institutes of Health Research (CIHR) and the British Columbia and Yukon Heart and Stroke Foundation of Canada. W.W.W. is a scholar of the Michael Smith Foundation for Health Research and is supported by the CIHR. M.R.H. is a University Killam Professor and holds a Canada Research Chair in Human Genetics.

REFERENCES

1. Fielding, C. J., and P. E. Fielding. 1995. Molecular physiology of reverse cholesterol transport. *J. Lipid Res.* **36:** 211–228.
2. Brooks-Wilson, A., M. Marcil, S. M. Clee, L. H. Zhang, K. Roomp, M. van Dam, L. Yu, C. Brewer, J. A. Collins, H. O. Molhuizen, et al. 1999. Mutations in ABC1 in Tangier disease and familial high-density lipoprotein deficiency. *Nat. Genet.* **22:** 336–345.
3. Bodzioch, M., E. Orso, J. Klucken, T. Langmann, A. Bottcher, W. Diederich, W. Drobnik, S. Barlage, C. Buchler, M. Porsch-Ozcurumez, et al. 1999. The gene encoding ATP-binding cassette transporter 1 is mutated in Tangier disease. *Nat. Genet.* **22:** 347–351.
4. Rust, S., M. Rosier, H. Funke, J. Real, Z. Amoura, J. C. Piette, J. F. Deleuze, H. B. Brewer, N. Duverger, P. Denefle, et al. 1999. Tangier disease is caused by mutations in the gene encoding ATP-binding cassette transporter 1. *Nat. Genet.* **22:** 352–355.
5. Clee, S. M., J. J. Kastelein, M. van Dam, M. Marcil, K. Roomp, K. Y. Zwarts, J. A. Collins, R. Roelants, N. Tamasawa, T. Stulc, et al. 2000. Age and residual cholesterol efflux affect HDL cholesterol levels and coronary artery disease in ABCA1 heterozygotes. *J. Clin. Invest.* **106:** 1263–1270.
6. Hayden, M. R., S. M. Clee, A. Brooks-Wilson, J. Genest, Jr., A. Attie, and J. J. Kastelein. 2000. Cholesterol efflux regulatory protein, Tangier disease and familial high-density lipoprotein deficiency. *Curr. Opin. Lipidol.* **11:** 117–122.
7. Schmitz, G., and T. Langmann. 2001. Structure, function and regulation of the ABC1 gene product. *Curr. Opin. Lipidol.* **12:** 129–140.
8. Wang, N., D. L. Silver, C. Thiele, and A. R. Tall. 2001. ATP-binding cassette transporter A1 (ABCA1) functions as a cholesterol efflux regulatory protein. *J. Biol. Chem.* **276:** 23742–23747.
9. Luciani, M. F., and G. Chimini. 1996. The ATP binding cassette transporter ABC1 is required for the engulfment of corpses generated by apoptotic cell death. *EMBO J.* **15:** 226–235.
10. Van Eck, M., I. S. Bos, W. E. Kaminski, E. Orso, G. Rothe, J. Twisk, A. Bottcher, E. S. Van Amersfoort, T. A. Christiansen-Weber, W. P. Fung-Leung, et al. 2002. Leukocyte ABCA1 controls susceptibility to atherosclerosis and macrophage recruitment into tissues. *Proc. Natl. Acad. Sci. USA.* **99:** 6298–6303.
11. Hamon, Y., M. F. Luciani, F. Becq, B. Verrier, A. Rubartelli, and G. Chimini. 1997. Interleukin-1beta secretion is impaired by inhibitors of the ATP binding cassette transporter, ABC1. *Blood.* **90:** 2911–2915.
12. Wellington, C. L., E. K. Walker, A. Suarez, A. Kwok, N. Bissada, R. Singaraja, Y. Z. Yang, L. H. Zhang, E. James, J. E. Wilson, et al. 2002. ABCA1 mRNA and protein distribution patterns predict multiple different roles and levels of regulation. *Lab. Invest.* **82:** 273–283.
13. Langmann, T., J. Klucken, M. Reil, G. Liebisch, M. F. Luciani, G. Chimini, W. E. Kaminski, and G. Schmitz. 1999. Molecular cloning of the human ATP-binding cassette transporter 1 (hABC1): evidence for sterol-dependent regulation in macrophages. *Biochem. Biophys. Res. Commun.* **257:** 29–33.
14. Oram, J. F. 2002. Molecular basis of cholesterol homeostasis: lessons from Tangier disease and ABCA1. *Trends Mol. Med.* **8:** 168–173.
15. Wellington, C. L., L. R. Brunham, S. Zhou, R. R. Singaraja, H. Visscher, A. Gelfer, C. Ross, E. James, G. Liu, M. T. Huber, et al. 2003. Alterations of plasma lipids in mice via adenoviral-mediated hepatic overexpression of human ABCA1. *J. Lipid Res.* **44:** 1470–1480.
16. Basso, F., L. Freeman, C. L. Knapper, A. Remaley, J. Stonik, E. B. Neufeld, T. Tansey, M. J. Amar, J. Fruchart-Najib, N. Duverger, et al. 2003. Role of the hepatic ABCA1 transporter in modulating intrahepatic cholesterol and plasma HDL cholesterol concentrations. *J. Lipid Res.* **44:** 296–302.
17. Timmins, J. M., J-Y. Lee, E. Boudyguina, K. Kluckman, L. R. Brunham, A. Mulya, A. K. Gebre, J. Coutinho, P. L. Colvin, T. L. Smith, et al. 2005. Targeted inactivation of hepatic ABCA1 causes profound hypoalphalipoproteinemia and kidney hypercatabolism of apolipoprotein A-I. *J. Clin. Invest.* Epub ahead of print. April 7, 2005. doi.: 10.1172/JCI200523915.
18. Haghpassand, M., P. A. Bourassa, O. L. Francone, and R. J. Aiello. 2001. Monocyte/macrophage expression of ABCA1 has minimal contribution to plasma HDL levels. *J. Clin. Invest.* **108:** 1315–1320.
19. Aiello, R. J., D. Brees, P. A. Bourassa, L. Royer, S. Lindsey, T. Coskran, M. Haghpassand, and O. L. Francone. 2002. Increased atherosclerosis in hyperlipidemic mice with inactivation of ABCA1 in macrophages. *Arterioscler. Thromb. Vasc. Biol.* **22:** 630–637.
20. Singaraja, R. R., V. Bocher, E. R. James, S. M. Clee, L. H. Zhang, B. R. Leavitt, B. Tan, A. Brooks-Wilson, A. Kwok, N. Bissada, et al. 2001. Human ABCA1 BAC transgenic mice show increased high density lipoprotein cholesterol and apoAI-dependent efflux stimulated by an internal promoter containing liver X receptor response elements in intron 1. *J. Biol. Chem.* **276:** 33969–33979.
21. Singaraja, R. R., C. Fievet, G. Castro, E. R. James, N. Hennuyer, S. M. Clee, N. Bissada, J. C. Choy, J. C. Fruchart, B. M. McManus, et al. 2002. Increased ABCA1 activity protects against atherosclerosis. *J. Clin. Invest.* **110:** 35–42.
22. Vaisman, B. L., G. Lambert, M. Amar, C. Joyce, T. Ito, R. D. Shamburek, W. J. Cain, J. Fruchart-Najib, E. D. Neufeld, A. T. Remaley, et al. 2001. ABCA1 overexpression leads to hyperalphalipoproteinemia and increased biliary cholesterol excretion in transgenic mice. *J. Clin. Invest.* **108:** 303–309.
23. Joyce, C. W., M. J. Amar, G. Lambert, B. L. Vaisman, B. Paigen, J. Najib-Fruchart, R. F. Hoyt, Jr., E. D. Neufeld, A. T. Remaley, D. S. Fredrickson, et al. 2002. The ATP binding cassette transporter A1

(ABCA1) modulates the development of aortic atherosclerosis in C57BL/6 and apoE-knockout mice. *Proc. Natl. Acad. Sci. USA.* **99:** 407–412.
24. Joyce, C., L. Freeman, H. B. Brewer, Jr., and S. Santamarina-Fojo. 2003. Study of ABCA1 function in transgenic mice. *Arterioscler. Thromb. Vasc. Biol.* **23:** 965–971.
25. McNeish, J., R. J. Aiello, D. Guyot, T. Turi, C. Gabel, C. Aldinger, K. L. Hoppe, M. L. Roach, L. J. Royer, J. de Wet, et al. 2000. High density lipoprotein deficiency and foam cell accumulation in mice with targeted disruption of ATP-binding cassette transporter-1. *Proc. Natl. Acad. Sci. USA.* **97:** 4245–4250.
26. Cavelier, L. B., Y. Qiu, J. K. Bielicki, V. Afzal, J. F. Cheng, and E. M. Rubin. 2001. Regulation and activity of the human ABCA1 gene in transgenic mice. *J. Biol. Chem.* **276:** 18046–18051.
27. Barter, P. J., H. B. Brewer, Jr., M. J. Chapman, C. H. Hennekens, D. J. Rader, and A. R. Tall. 2003. Cholesteryl ester transfer protein: a novel target for raising HDL and inhibiting atherosclerosis. *Arterioscler. Thromb. Vasc. Biol.* **23:** 160–167.
28. Yanai, I., D. Graur, and R. Ophir. 2004. Incongruent expression profiles between human and mouse orthologous genes suggest widespread neutral evolution of transcription control. *OMICS.* **8:** 15–24.
29. Wagner, A. 2000. Decoupled evolution of coding region and mRNA expression patterns after gene duplication: implications for the neutralist-selectionist debate. *Proc. Natl. Acad. Sci. USA.* **97:** 6579–6584.
30. Cheung, C., T. E. Akiyama, J. M. Ward, C. J. Nicol, L. Feigenbaum, C. Vinson, and F. J. Gonzalez. 2004. Diminished hepatocellular proliferation in mice humanized for the nuclear receptor peroxisome proliferator-activated receptor alpha. *Cancer Res.* **64:** 3849–3854.
31. Sarsero, J. P., L. Li, T. P. Holloway, L. Voullaire, S. Gazeas, K. J. Fowler, D. M. Kirby, D. R. Thorburn, A. Galle, S. Cheema, et al. 2004. Human BAC-mediated rescue of the Friedreich ataxia knockout mutation in transgenic mice. *Mamm. Genome.* **15:** 370–382.
32. Chen, J. Y., B. Levy-Wilson, S. Goodart, and A. D. Cooper. 2002. Mice expressing the human CYP7A1 gene in the mouse CYP7A1 knock-out background lack induction of CYP7A1 expression by cholesterol feeding and have increased hypercholesterolemia when fed a high fat diet. *J. Biol. Chem.* **277:** 42588–42595.
33. Kent, W. J., C. W. Sugnet, T. S. Furey, K. M. Roskin, T. H. Pringle, A. M. Zahler, and D. Haussler. 2002. The human genome browser at UCSC. *Genome Res.* **12:** 996–1006.
34. Sandelin, A., W. W. Wasserman, and B. Lenhard. 2004. ConSite: web-based prediction of regulatory elements using cross-species comparison. *Nucleic Acids Res.* **32:** W249–W252.
35. Kolbe, D., J. Taylor, L. Elnitski, P. Eswara, J. Li, W. Miller, R. Hardison, and F. Chiaromonte. 2004. Regulatory potential scores from genome-wide three-way alignments of human, mouse, and rat. *Genome Res.* **14:** 700–707.
36. Lenhard, B., A. Sandelin, L. Mendoza, P. Engstrom, N. Jareborg, and W. W. Wasserman. 2003. Identification of conserved regulatory elements by comparative genome analysis. *J. Biol.* **2:** 13.
37. Willy, P. J., K. Umesono, E. S. Ong, R. M. Evans, R. A. Heyman, and D. J. Mangelsdorf. 1995. LXR, a nuclear receptor that defines a distinct retinoid response pathway. *Genes Dev.* **9:** 1033–1045.
38. Sandelin, A., and W. W. Wasserman. 2004. Prediction of nuclear hormone receptor response elements. *Mol. Endocrinol.* **19:** 595–606.
39. Lowry, O. H., N. J. Rosebrough, A. L. Farr, and R. J. Randall. 1951. Protein measurement with the Folin phenol reagent. *J. Biol. Chem.* **193:** 265–275.
40. Twisk, J., D. L. Gillian-Daniel, A. Tebon, L. Wang, P. H. Barrett, and A. D. Attie. 2000. The role of the LDL receptor in apolipoprotein B secretion. *J. Clin. Invest.* **105:** 521–532.
41. Wasserman, W. W., and A. Sandelin. 2004. Applied bioinformatics for the identification of regulatory elements. *Nat. Rev. Genet.* **5:** 276–287.
42. Santamarina-Fojo, S., K. Peterson, C. Knapper, Y. Qiu, L. Freeman, J. F. Cheng, J. Osorio, A. Remaley, X. P. Yang, C. Haudenschild, et al. 2000. Complete genomic sequence of the human ABCA1 gene: analysis of the human and mouse ATP-binding cassette A promoter. *Proc. Natl. Acad. Sci. USA.* **97:** 7987–7992.
43. Wasserman, W. W., M. Palumbo, W. Thompson, J. W. Fickett, and C. E. Lawrence. 2000. Human-mouse genome comparisons to locate regulatory sites. *Nat. Genet.* **26:** 225–228.
44. Costet, P., Y. Luo, N. Wang, and A. R. Tall. 2000. Sterol-dependent transactivation of the ABC1 promoter by the liver X receptor/retinoid X receptor. *J. Biol. Chem.* **275:** 28240–28245.
45. Grefhorst, A., B. M. Elzinga, P. J. Voshol, T. Plosch, T. Kok, V. W. Bloks, F. H. van der Sluijs, L. M. Havekes, J. A. Romijn, H. J. Verkade, et al. 2002. Stimulation of lipogenesis by pharmacological activation of the liver X receptor leads to production of large, triglyceride-rich very low density lipoprotein particles. *J. Biol. Chem.* **277:** 34182–34190.
46. Quinet, E. M., D. A. Savio, A. R. Halpern, L. Chen, C. P. Miller, and P. Nambi. 2004. Gene-selective modulation by a synthetic oxysterol ligand of the liver X receptor. *J. Lipid Res.* **45:** 1929–1942.
47. Qiu, Y., L. Cavelier, S. Chiu, X. Yang, E. Rubin, and J. F. Cheng. 2001. Human and mouse ABCA1 comparative sequencing and transgenesis studies revealing novel regulatory sequences. *Genomics.* **73:** 66–76.
48. Levy, S., and S. Hannenhalli. 2002. Identification of transcription factor binding sites in the human genome sequence. *Mamm. Genome.* **13:** 510–514.
49. Quack, M., C. Frank, and C. Carlberg. 2002. Differential nuclear receptor signalling from DR4-type response elements. *J. Cell. Biochem.* **86:** 601–612.
50. Willy, P. J., and D. J. Mangelsdorf. 1997. Unique requirements for retinoid-dependent transcriptional activation by the orphan receptor LXR. *Genes Dev.* **11:** 289–298.
51. Wang, N., W. Chen, P. Linsel-Nitschke, L. O. Martinez, B. Agerholm-Larsen, D. L. Silver, and A. R. Tall. 2003. A PEST sequence in ABCA1 regulates degradation by calpain protease and stabilization of ABCA1 by apoA-I. *J. Clin. Invest.* **111:** 99–107.
52. Tornell, J., and M. Snaith. 2002. Transgenic systems in drug discovery: from target identification to humanized mice. *Drug Discov. Today.* **7:** 461–470.
53. Moriguchi, T., H. Motohashi, T. Hosoya, O. Nakajima, S. Takahashi, S. Ohsako, Y. Aoki, N. Nishimura, C. Tohyama, Y. Fujii-Kuriyama, et al. 2003. Distinct response to dioxin in an arylhydrocarbon receptor (AHR)-humanized mouse. *Proc. Natl. Acad. Sci. USA.* **100:** 5652–5657.
54. Masson, D., B. Staels, T. Gautier, C. Desrumaux, A. Athias, N. Le Guern, M. Schneider, Z. Zak, L. Dumont, V. Deckert, et al. 2004. Cholesteryl ester transfer protein modulates the effect of liver X receptor agonists on cholesterol transport and excretion in the mouse. *J. Lipid Res.* **45:** 543–550.